IOMAC'19
8th International Operational Modal Analysis Conference
2019 May13-15 Copenhagen

OMA-BASED STRUCTURAL HEALTH MONITORING OF A WOODEN MAST STRUCTURE EXPOSED TO AMBIENT VIBRATIONS

Pernille Lysgaard Andersen[1], *Silja Tea Nielsen*[2], *Sandro D. R. Amador*[3], *Evangelos Katsanos*[4] *and Rune Brincker*[5]

[1] Student, Technical University of Denmark (DTU), Department of Civil Engineering, pernille@lysgaard-andersen.dk.
[2] Student, Technical University of Denmark (DTU), Department of Civil Engineering, siljatea@gmail.com.
[3] Assistant Professor, Technical University of Denmark (DTU), Department of Civil Engineering, sdio@byg.dtu.dk.
[4] Assistant Professor, Technical University of Denmark (DTU), Department of Civil Engineering, vakat@byg.dtu.dk.
[5] Professor, Technical University of Denmark (DTU), Department of Civil Engineering, runeb@byg.dtu.dk.

ABSTRACT
OMA-based Structural Health Monitoring (SHM) relies on the modal parameters in order to identify the health condition of a structure. These parameters are affected both by structural changes and the varying environmental/operational conditions. In order to robustly detect structural modifications in the monitored structures, an OMA-based SHM approach must distinguish between the different sources of change. Along these lines, this study aims at detecting structural changes in a structure subjected to varying environmental conditions. The investigated structure consists of a wooden mast and a steel frame top site, and is monitored by a modern vibration-based acquisition system while a weather station captures the environmental conditions. The measurements provided are used to: establish an environmental model for the mast structure; remove the effect of the environmental conditions from the estimated modal parameters and finally detect structural changes such as induced damages, hereby assessing the efficiency of the deployed OMA-based SHM approach.

Keywords: Operational Modal Analysis, Structural Health Monitoring, Changing environmental/operational conditions, Damage detection

1. INTRODUCTION

Critical infrastructures including road networks, bridges, energy plants, and power grids as well as ports, marine, and offshore facilities are structural systems of increased importance for the welfare and sustainable development of modern societies. Therefore, securing the safe operation and structural integrity of those structural systems should be highly prioritised. This is often pursued by surveying

the structural systems with human-driven inspections and rather ad hoc monitoring campaigns. These methods can be associated with significant time and monetary burden while the reliability can be adversely affected by human errors. Demanding challenges need also to be met in case of monitoring hardly accessible structures. Therefore, robust techniques should be adopted to perform structural health monitoring (SHM) on a continuous, systematic and reliable basis.

Numerous SHM methods have been already proposed in the literature. Measuring structural vibrations and consequently identifying the modal properties in form of the natural frequencies, damping ratios and mode shapes of a structure constitute a widely used framework to assess the health of a monitored structure [1, 2]. Within this framework, operational modal analysis (OMA) can accommodate the purposes of monitoring a structure while in operation [3, 4]. The choice of an identification technique, which enables a reliable and stable estimation of the modal properties, is of high relevance for SHM campaigns. Moreover, continuity of the vibration-based monitoring requires automation of OMA and the pertinent modal identification. This can be problematic, especially in cases where noise-related modes interfere extensively with the physical ones [5]. Reliable application of the OMA-based SHM methods also relies on identifying and then, eliminating the influence of the environmental and operational (e.g., temperature, moisture and wind speed) variability (EOV) on the modal properties [2, 5, 6]. Various methods have been already used to lessen the EOV effects on the modal properties including models that follow the principal component analysis [2, 7], multivariate linear regression [8], and auto regressive models [9, 10]. One full year is commonly considered as a reasonable time frame to estimate reliable EOV models; however, time restrictions have led researchers to perform the essential EOV-based correction of the identified modal properties by using data obtained after a few months of monitoring [1, 9]. The meticulous design and installation of the measurement system as well as the establishment of quality assurance criteria for the monitoring data can further increase reliability of any SHM campaign [11]. Ultimately, all of these refinements allow SHM to be applied for damage detection [7, 9, 12, 13].

As can be seen from the above many advancements have been already made in SHM, however for the present study it is chosen to deliberately avoid a highly complex SHM scheme. This allows for a transparent investigation of how the different parts of the SHM scheme affects the final outcome. Along these lines, the present experimental study focuses on utilizing a state-of-the-art OMA technique on an automated basis in order to monitor the health of a medium-sized wooden mast with a top mass subjected to wind-induced load. The experimental model is placed in an outdoor environment and thus, it is necessary to develop an EOV model in order to eliminate the influence of EOV on the modal properties. The measuring system is designed with contemporary sensors and the quality of the measurements as well as the performance of the identification technique are continuously evaluated during the 32 day long monitoring campaign. Moreover, damages are induced to the wooden mast to investigate whether the detection of those structural changes is feasible by the designed SHM system. The objectives of this study are briefly described below:

- experimental identification of natural frequencies of the wooden mast in order to detect deliberately induced damages
- evaluation of the quality and reliability of the monitoring data used for the modal identification
- application of an environmental model to eliminate the effects of EOV on the identified natural frequencies

2. METHODOLOGY

The theoretical background and methodology applied for the SHM scheme are described in this section. This includes description of the time domain poly reference (TDPR) identification technique, the environmental model used to correct the identified natural frequencies, and the damage detection procedure.

2.1. Identification by Time Domain Poly Reference

The TDPR is an autoregression (AR) based identification technique where an AR model is fitted to the correlation functions (CFs) of the structural response, as these can be interpreted as free decays. The AR model is described at the discrete time instant n by the difference equation

$$\mathbf{y}(n) - \mathbf{A}_1\mathbf{y}(n-1) - \mathbf{A}_2\mathbf{y}(n-2) - ... - \mathbf{A}_{na}\mathbf{y}(n-na) = \mathbf{0} \tag{1}$$

where $\mathbf{y}(n)$ holds nc free decays with np number of samples and na is the number of previous time instances to include in the consideration. $\mathbf{A}_k$ is the AR matrices to be estimated, which is accomplished by setting up an overdetermined system with $np - na$ set of equations and performing least square regression defined by

$$\mathbf{A}\mathbf{H}_1 = \mathbf{H}_2 \qquad \Leftrightarrow \qquad \hat{\mathbf{A}} = \mathbf{H}_2\mathbf{H}_1^+ \tag{2}$$

where $[\cdot]^+$ denotes the pseudo-inverse and $\mathbf{A}$ holds the AR matrices $\mathbf{A} = [\mathbf{A}_{na},\ \mathbf{A}_{na-1},\ \ldots,\ \mathbf{A}_1]$. $\mathbf{H}_1$ and $\mathbf{H}_2$ are Hankel block matrices, set up as

$$\mathbf{H}_1 = \begin{bmatrix} \mathbf{y}(1) & \mathbf{y}(2) & \ldots & \mathbf{y}(np-na) \\ \mathbf{y}(2) & \mathbf{y}(3) & \ldots & \mathbf{y}(np-(na-1)) \\ \vdots & \vdots & \ddots & \vdots \\ \mathbf{y}(na) & \mathbf{y}(na+1) & \ldots & \mathbf{y}(np-1) \end{bmatrix},\ \mathbf{H}_2 = \begin{bmatrix} \mathbf{y}(na+1) & \mathbf{y}(na+2) & \ldots & \mathbf{y}(np) \end{bmatrix} \tag{3}$$

The difference equation given in Equation (1) is reformulated to a state space formulation containing the companion matrix, and the modal parameters are then determined by eigenvalue decomposition of this companion matrix. A more detailed description of the applied TDPR technique is provided by [14].

The CFs are found by first determining the spectral densities (SDs) with the use of the Welch averaging technique with 50% overlap and by convolution. A band-pass frequency domain window is applied to the SDs to keep a narrow band of frequencies only containing modes of the structure close to each other. The identification procedure is thus split up in several narrow band analyses of grouped modes, as this minimises disturbance from noise modes. The CFs are then estimated by taking the SDs back to the time domain through inverse fast fourier transform. To avoid bias from noise in the beginning of the CFs and the noise tail, only the intermediate part of the CFs are applied for identification. Optimized condensation of the CFs are implemented to pick out the physical modes from the noise modes. This is accomplish by following the procedure presented in [15]. By applying condensation it is necessary to request and therefore know the number of physical modes in each frequency band. nr number of CFs are gathered in $\mathbf{Y} = [\mathbf{y}_1(n),\ \mathbf{y}_2(n), \ldots,\ \mathbf{y}_{nr}(n)]$ and used as the input in the Hankel block matrices given in (3) with $na = 2$ block rows. The size of $\mathbf{Y}$ is $nc \times nr = 6 \times 6$ and the number of samples is different in each analysis of grouped modes but is at least $np = 256$ why the system is well overdetermined to obtain a satisfactory estimate of the AR matrices, $\hat{\mathbf{A}}$.

2.2. Environmental Model

In order to describe the effect from the EOV on the natural frequencies, an environmental model is established by fitting a set of predictors, p_j, to the identified natural frequency of each mode, n. This is accomplished by performing multivariate linear least squares regression. The linear regression model to predict the natural frequencies, $\hat{f}_n$, is described as

$$\hat{f}_n(p_j(t)) = \beta_{0,n} + \sum_{j=1}^{J} \beta_{j,n} p_j(t) \tag{4}$$

where β are the regression coefficients, estimated by setting up a matrix equation and performing least square regression as

$$\mathbf{f}_n = \mathbf{P}\boldsymbol{\beta}_n \qquad \Leftrightarrow \qquad \hat{\boldsymbol{\beta}}_n = \mathbf{P}^{+}\mathbf{f}_n \tag{5}$$

where $\boldsymbol{\beta}_n$ holds the regression coefficients, $\mathbf{P}$ contain the predictors for all time instances, i, and the identified natural frequency at each instance, i, are located in $\mathbf{f}_n$. The environmental model can account for several parameters, herein air temperature, relative humidity, wind speed, and wind direction are investigated. The environmental parameters are averaged over the measurement duration in order to be applied as predictors. Cross terms of these predictors are applied as well. To determine the optimal model and set of predictors, a 80/20 percent split of data from the healthy structure is applied to obtain a training and a test set respectively. The optimal model is chosen based on a balance between its predicting abilities in the test set and simplicity. The predicting ability is evaluated through the root mean square (rms) error.

2.3. Damage Detection

In this study, damage detection is based on the natural frequencies estimated at each time instance, i, and corrected in order to minimize the influence from the environmental conditions. The corrected natural frequencies, f_n^c, are determined as

$$f_{i,n}^c = \mathrm{M}[f_n] + \varepsilon_{i,n} \qquad \text{where} \qquad \varepsilon_i = f_{i,n} - \hat{f}_{i,n} \tag{6}$$

where $\mathrm{M}[\cdot]$ is the median operator applied on the identified natural frequencies from the healthy test data set. The mean value of the corrected frequencies are expected to be constant as long as the structure is healthy while changes from the mean indicate damage. The definition of damage detection applied here is therefore based on statistical process control, where a value outside a band around the mean value is defined as an outlier. Previous studies apply different control limits, for example, in [10, 13] the boundaries of a 95% confidence interval are used, which corresponds to a deviation of two times the standard deviation from the mean value. A factor of three times the standard deviation corresponds to a 99.7% confidence level. Instead of creating the limits based on standard deviation and the mean value, it is chosen to construct them from median absolute deviation (MAD) value, due to a limited amount of data [16]. The control limits of each mode, L_n, are defined by

$$L_n = \mathrm{M}[f_n] \pm 3 \cdot \mathrm{MAD}_n \qquad \text{where} \qquad \mathrm{MAD}_n = 1.4826 \cdot \mathrm{M}[f_n^c - \mathrm{M}[f_n^c]] \tag{7}$$

Chosing a factor of three on the deviation measure is considered conservative [16], meaning that it leads to a seldom but expected occurrence of outliers (values outside of these limits). Therefore, the final decision taken herein for defining the damage detection criterion is the following: the indication of a damage-related change in the median value of the natural frequencies corresponds to a continuity of outliers.

3. TEST SET-UP

The monitored experimental model is a medium sized monopile-like structure consisting of a 3.6 m high wooden mast with a square cross section of 0.1 m $\times$ 0.1 m, see Figure 1. A steel girder is placed at the top of the mast and it is founded rigidly on a concrete block. The connections at the base and the top are both carried out as bolted steel connections while they are deliberately designed to host realistic imperfections. The model is placed outside lab facilities, thus it is exposed to natural loads mainly related to wind-induced lateral loads. The sensors used for measuring the structural response are triaxial geophones, chosen for their high sensitivity and low noise floor. Three of these sensors are placed on the corners of the top site as presented in Figure 1 (top right). The measured corner displacements (x_j, y_j, z_j) are converted into the three translational (x_c, y_c, z_c) and three rotational $(\theta_{x,c}, \theta_{y,c}, \theta_{z,c})$ degrees of freedom

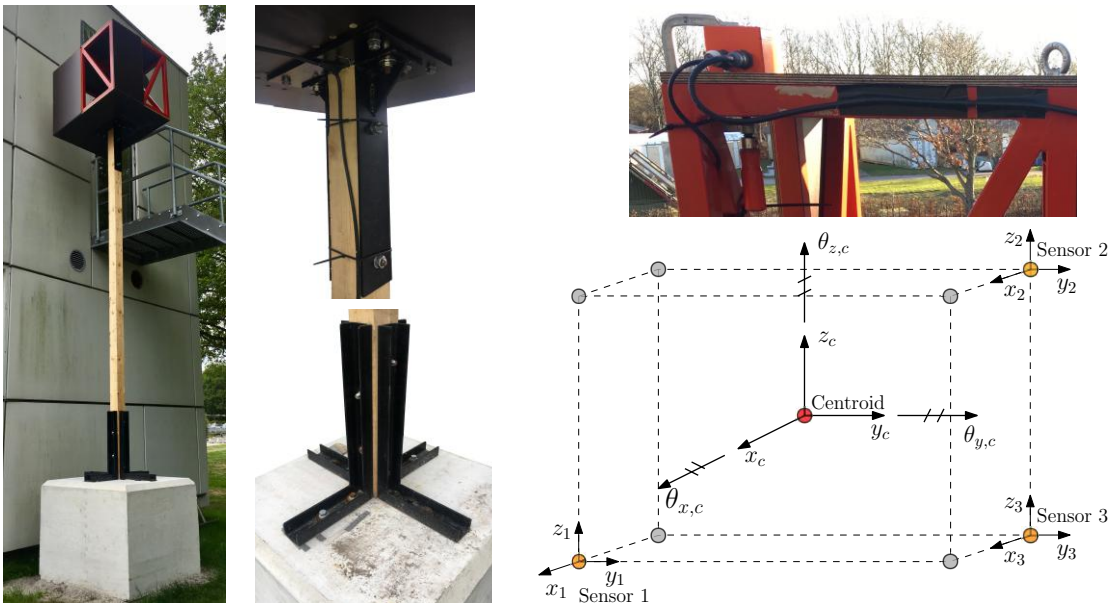

Figure 1: Left: Photo of the experimental model. Middle: Photos of connections. Top right: Sensor mounting with clamp, strips and tape. Bottom right: Diagram of top site with the sensor placements shown with orange dots. The nine corner directions and six centroid DOFs are shown with arrows.

(DOFs) at the centroid of the top site illustrated in Figure 1 (bottom right). This transformation is achieved by considering rigid body movements of the top site.

The monitoring campaign is initiated at 2018/10/03 and finalised at 2018/11/05 while measurements are performed on an hourly basis with a sampling frequency of $f_s = 100$Hz and a duration of $T = 1200$s. The damage is initially induced at 2018/10/30. Three different filters are applied to the measurments in the frequency domain, one for integration (i.e., from velocity to displacement time series), one for correction of the dynamic system of the geophone per se, and one for filtering out frequencies below 0.5Hz and above 25Hz. Additional information on the test set-up and signal processing can be found in [17].

4. QUALITY ASSESSMENT OF MEASUREMENTS

A representative example of the measured signals is presented in Figure 2 (left) as the singular value plot of the SD matrix. To approach robust and reliable monitoring campaign, the quality of each measurement is assessed prior to its use for identification purposes. The quality is assessed based on two parameters: A residual measure accounting for the transformation from the corner signals to the centroid DOFs and the signal to noise ratio (SNR) of the measurement. As it concerns the first parameter, the residual value indicates errors in the recorded signal as it detects discrepancy between the recorded and estimated signals. Furthermore, the SNR must be high to ensure that the physics are clearly represented in the measurement. By applying appropriate thresholds, measurements with signal errors and low SNR are discarded. More details about the applied thresholds can be found in [17]. The evaluation of all measurements is presented in Figure 2 (right), where it can be seen that a total of five measurements are discarded. However, an additional measurement was removed due to manual detection of a signal error, thus the presented quality assessment is incomplete. In total 99.1% of measurements are of sufficient quality to be used for identification.

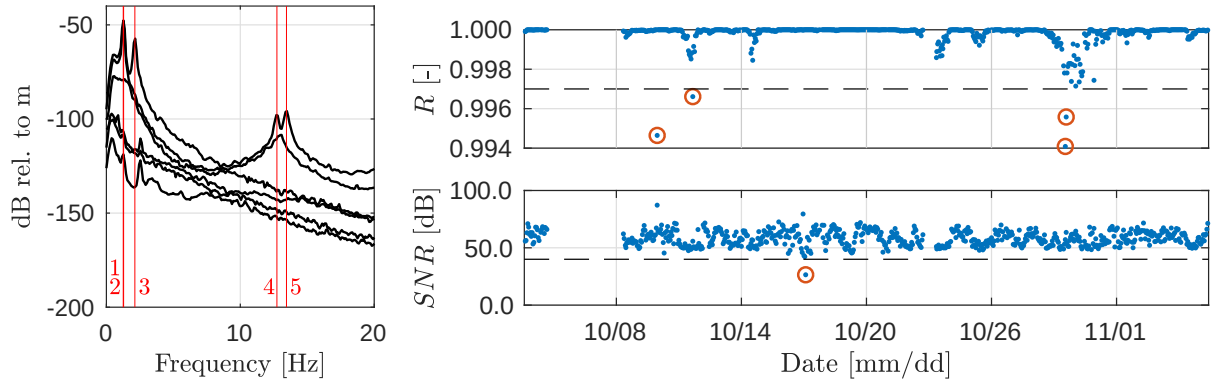

Figure 2: Left: Singular value plot of the spectral density of the signal after signal processing with indication of the first five modes (|). Right: Quality assessment values shown for all measurements (•), shown with the chosen threshold (−−) and indication of discarded measurements (○)

5. RESULTS

The SHM scheme adopted herein and the assosiated results follow the methodology presented in section 2. Therefore, results concerning the system identification, the environmental model, and the final damage detection are described in the following sections. `Matlab` [18] is utilised to perform relevant calculations.

5.1. Identified Modal Parameters

The signals used for modal identification is presented by an example in Figure 2 (left). It can be seen that the three first modes (i.e., the first two bending modes and the first torsional one) are adjacent ones (i.e., 1.26Hz to 2.13Hz) while such a modal proximity can also be detected for the second couple of bending modes (i.e., 12.7Hz to 13.4Hz). The latter allows for creating two modal groups for identification, containing modes 1-3 and 4-5 respectively. The identified natural frequencies, damping ratios, and pertinent mode shapes are presented in Figure 3 to exemplify the monitoring results. As the identified mode shapes tend to mix with other mode shapes in their proximity, these are separated by projecting the direction of a mode onto a subspace of identified modes. This is done according to [14] by

$$\mathbf{a}_{p,n} = \mathbf{A}\hat{\mathbf{t}} \qquad \text{where} \qquad \hat{\mathbf{t}} = \mathbf{A}^{+}\mathbf{b}_n \tag{8}$$

where $\mathbf{a}_{p,n}$ is the projected mode shape vector, $\mathbf{A}$ is a subspace of mixing modes shapes and $\mathbf{b}_n$ is the direction vector for the n^{th} mode. The direction vectors are applied as rough estimates with values of unity placed at the DOFs in $\mathbf{b}_n$ that are expected to be activated for each mode. In [17] it is shown that the projected mode shape, $\mathbf{a}_{p,n}$, is not affected by the rough estimate of $\mathbf{b}_n$ as long as $\mathbf{b}_n$ contains values in the correct translational or rotational DOFs.

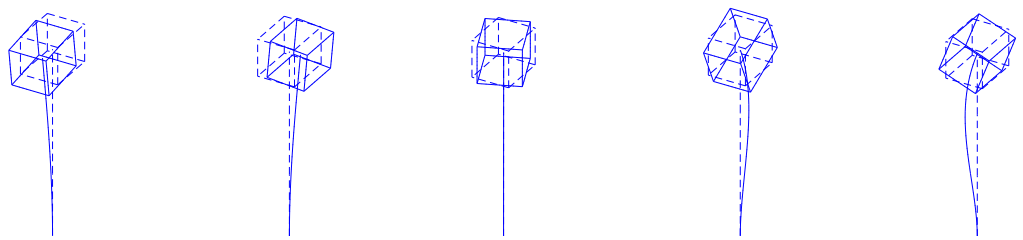

$f_1 = 1.26$ Hz, $\zeta_1 = 1.20$ %
$f_2 = 1.28$ Hz, $\zeta_2 = 0.81$ %
$f_3 = 2.13$ Hz, $\zeta_3 = 1.19$ %
$f_4 = 12.7$ Hz, $\zeta_4 = 0.84$ %
$f_5 = 13.4$ Hz, $\zeta_5 = 0.87$ %

Figure 3: Example of identified modal parameters from the measurement at 2018/10/15 16:00:07. The mode shapes, $\mathbf{a}_{p,n}$, are separated by projection and visualised by expansion to the wooden pile and the top site.

For illustrative purposes, the mode shapes presented in Figure 3 are expanded to include the geometry of the top site and wooden pile in addition to the top site centroid DOFs. This is accomplished by considering rigid body movements of the top site and polynomial formulation for the wooden mast deflections from foundation level $z = 0$ to the centroid of top site $z = L$ given as

$$\begin{bmatrix} x(z) \\ y(z) \end{bmatrix} = \begin{bmatrix} (L \cdot \theta_{y,c} - 2 \cdot x_c) \cdot z^3/L^3 - (L \cdot \theta_{y,c} - 3 \cdot x_c) \cdot z^2/L^2 \\ (L \cdot \theta_{x,c} - 2 \cdot y_c) \cdot z^3/L^3 - (L \cdot \theta_{x,c} - 3 \cdot y_c) \cdot z^2/L^2 \end{bmatrix} \tag{9}$$

where $L = 3.6 + 0.4$ m and $x_c,\ y_c,\ \theta_{x,c}$ and $\theta_{y,c}$ correspond to the centroid DOFs in the projected mode shapes $\mathbf{a}_{p,n}$.

The performance of the TDPR identification on a fully automated basis is considered successful as the first five modes of the experimental model are identified for all measurements available from the monitoring campaign after quality assessment. Based on this, the identification procedure is considered stable. The identified frequencies of the first mode prior to the EOV based correction can be seen in Figure 4 (top) considering all measurements taken from the healthy structure (prior to the deliberately induced damages). Daily patterns in the identified natural frequencies can be observed. Besides this variation no sudden outliers are found, thus the procedure can also be considered to be consistent.

5.2. Environmental Model

Preliminary analyses undertaken by the authors showed that the identified natural frequencies are strongly correlated with air temperature while less correlated with the additional environmental factors investigated; relative humidity of the air, wind speed, and wind direction. Figure 4 illustrates the changes of the first frequency in relation to the air temperature. As expected the natural frequencies decrease with increasing temperature. When correcting the frequencies based on the air temperature solely, the MAD value of the first-mode natural frequency in test data set decreases from 6.34mHz to 3.42mHz. When the additional environmental factors are considered, the corresponding MAD values are further reduced to 3.32mHz. However, such a minor change (from 3.42mHz to 3.32mHz) is found dispensable over the simplicity of developing the environmental model for the current SHM scheme based on air temperature only. Similar tendencies are observed for the remaining four modes thus the decision applies to all modes. The corrected frequencies of the first mode after application of the environmental model can be seen in Figure 4 (bottom). It should be mentioned that correction does not completely remove the daily, environmental-related pattern. Therefore, refinement of the environmental model should be pursued by using, e.g., a larger data set with measurements from a longer period of time or a dynamic modelling approach.

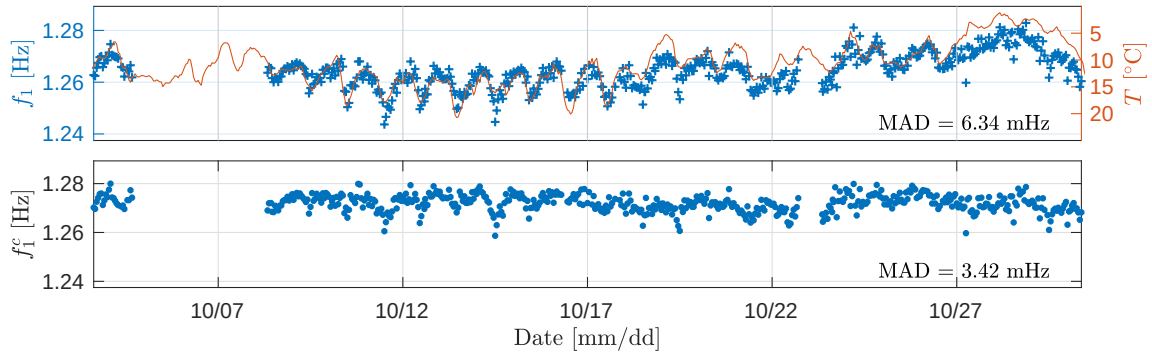

Figure 4: Measures for the first mode during the healthy structural state. Top: Identified natural frequency (+) and measured air temperature (–) . Bottom: Corrected natural frequencies (•) by the environmental model.

5.3. Damage Detection

Damage is induced to the wooden pile as eleven cuts near the foundation in six steps, as presented in Figure 5 and Table 1. The identified and environmentally corrected natural frequencies based on

measurements taken during the damage induction period are presented in Figure 6. It is seen that damage is indicated by continuous outliers already at the first damage step. The latter is more profound for the second mode while more convincing damage detection can be seen both for the first and second mode after the induction of the second damage step. On the other hand, the third mode is seen to be less sensi-

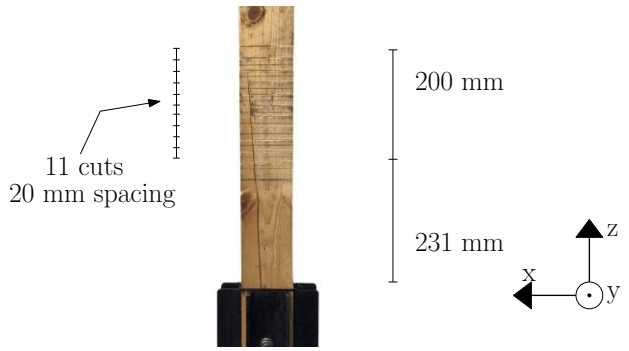

Figure 5: Illustration of the induced damages.

Table 1: Reduction of cross section for each damage step

Damage step	Reduction [%]
1	1.1
2	4.5
3	6.9
4	8.2
5	9.7
6	21.8

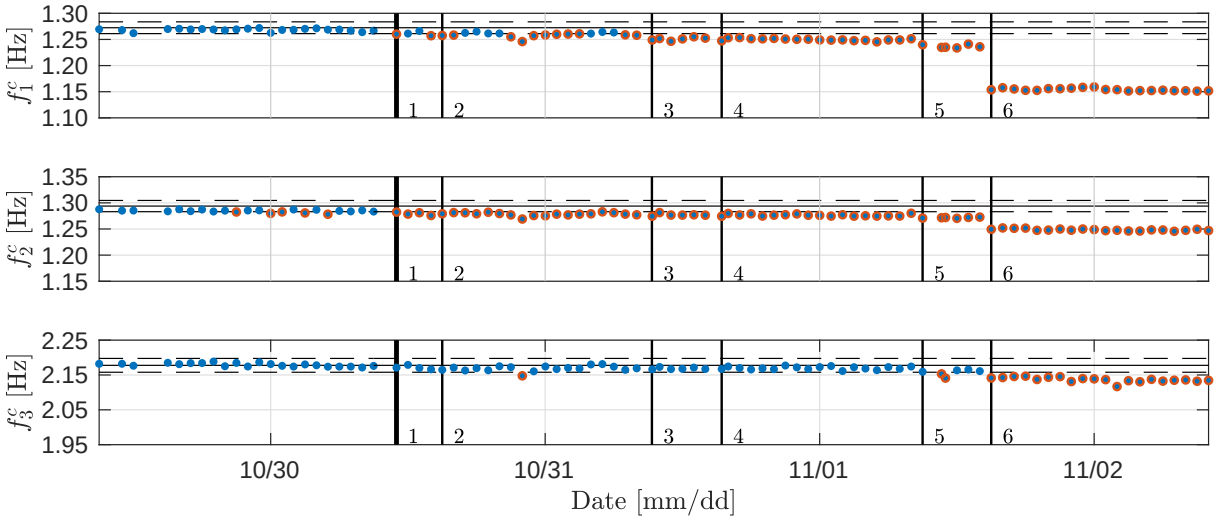

Figure 6: Corrected natural frequencies (•) at damaged structural state of the monitoring campaign. (○) indicates an outlier, (- -) is the control limits, (–) is the median and (|) indicates the damage step.

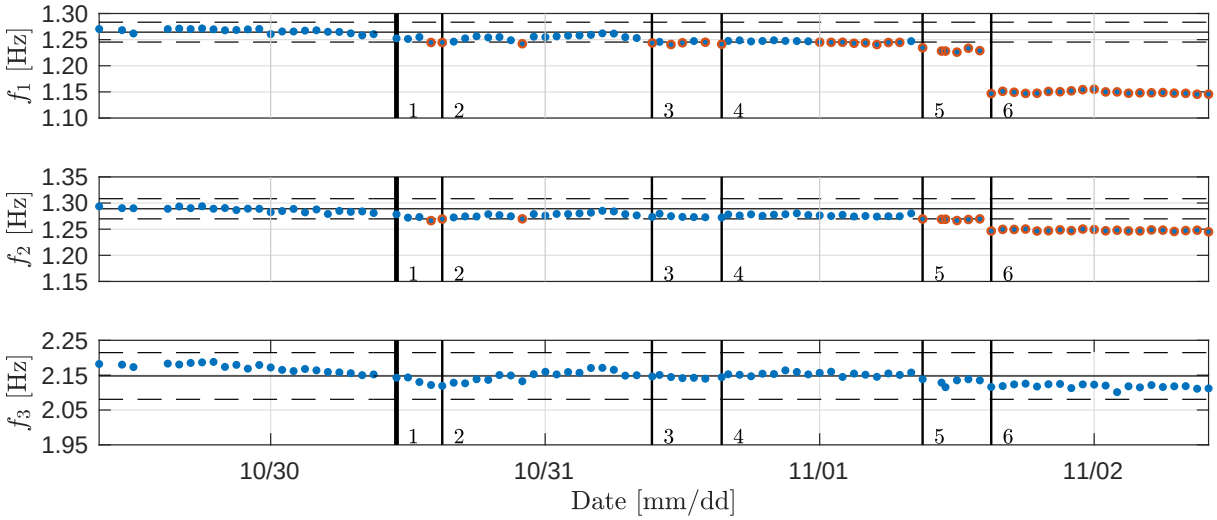

Figure 7: Natural frequencies (•) at damaged structural state of the monitoring campaign. (○) indicates an outlier, (- -) is the control limits, (–) is the median and (|) indicates the damage step.

tive to damage as only the last damage step (21.8% cross sectional reduction) can be identified. The high sensitivity of the first two modes is expected as the vibration profiles corresponding to these modes result in large bending moments close to the foundation, thus the location of the damage is critical for these modes. The rather noticeable decrease in the identified first-mode natural frequency after the last damage step can be explained by the fact that the induced damage reduces mostly the moment of inertia in the direction of the first mode.

Damage detection based on uncorrected frequencies is possible as well, as it can be seen from Figure 7. This indicates that the success of damage detection is not only a result of the temperature correction but also caused by reliability of the SHM and identification followed herein. However, the uncorrected frequencies are less sensitive to damage compared to the temperature corrected frequencies, as continuous outliers for the first and second-mode natural frequencies are first seen at the fourth and fifth damage step, respectively.

6. CONCLUSIONS

This study concerns a fully experimental application of SHM, in which detection of gradually induced damage close to the base of the wooden mast is attempted through identification of the first three natural frequencies. The results of the study show that

- deliberately induced damage is detected through pertinent changes in the natural frequencies
- when accounting for the effect of air temperature variability on the identified natural frequencies through a linear regression model, the natural frequencies show to be more sensitive to damage.
- 99.1% of measurements are found to be of satisfactory quality, while the TDPR identification technique succeeded for 100% of the measurements. Furthermore, the environmental model based on air temperature solely reduced the variability of the identified natural frequencies by 46%.

It is notable that the temperature correction applied in the present study is only based on 27 days of measurements. However, data describing the healthy structure over a longer time frame (i.e., a full year) are commonly considered to be necessary for developing a reliable environmental model. Therefore, the established environmental model may not facilitate long term forecasts despite the rather satisfactory performance that this model was found to have regarding correction of the identified natural frequencies. The latter can be considered beneficial when applying continuous updating of the environmental model in order to obtain reliable results within a short time frame. The quality assessment of the measurements showed to influence the success of identification, however refinement of the relevant criteria should be pursued while their automated performance may further increase the robustness of any SHM scheme.

ACKNOWLEDGEMENTS

The authors acknowledge the funding received from Centre for Oil and Gas - DTU/Danish Hydrocarbon Research and Technology Centre (DHRTC).

REFERENCES

[1] Rainieri, C., Gargaro, D. and Fabbrocino, G. (2015) Statistical tools for the characterization of environmental and operational factors in vibration-based SHM. In: *Structural Health Monitoring and Damage Detection*, 7, (pp. 175-184). Springer.

[2] Magalhães, F., Cunha, A. and Caetano, E. (2012) Vibration based structural health monitoring of an arch bridge: from automated OMA to damage detection. In: *Mechanical Systems and Signal Processing*, 28, (pp. 212-228). Elsevier.

[3] Weijtjens, W., Verbelen, T., Capello, E. and Devriendt, C. (2017) Vibration based structural health monitoring of the substructures of five offshore wind turbines. In: *Procedia engineering*, 199, (pp. 2294-2299). Elsevier.

[4] Peeters, B., Couvreur, G., Razinkov, O., Kündig, C., Van der Auweraer, H. and De Roeck, G. (2009) Continuous monitoring of the Øresund Bridge: system and data analysis. In: *Structures and Infrastructure Engineering*, 5(5), (pp. 392-405). Taylor & Francis.

[5] Carden, P.E. and Brownjohn, J. (2008) Fuzzy clustering of stability diagrams for vibration-based structural health monitoring. In: *Computer-Aided Civil and Infrastructure Engineering*, 23(5) (pp. 360-372). Wiley Online Library.

[6] Cross, E.J., Koo, K.Y., Brownjohn, J. and Worden, K. (2013) Long-term monitoring and data analysis of the Tamar Bridge. In: *Mechanical Systems and Signal Processing*, 35(1-2) (pp. 16-34). Elsevier.

[7] Diord, S., Magalhães, F., Cunha, A., Caetano, E. and Martins, N. (2017) Automated modal tracking in a football stadium suspension roof for detection of structural changes. In: *Structural Control and Health Monitoring*, 24(11) (pp. e2006). Wiley Online Library.

[8] Laory, I., Trinh, T.N., Smith, I.F.C and Brownjohn, J. (2014) Methodologies for predicting natural frequency variation of a suspension bridge. In: *Engineering Structures*, 80, (pp. 211-221). Elsevier.

[9] Peeters, B. and De Roeck, G. (2001) One-year monitoring of the Z24-Bridge: environmental effects versus damage events. In: *Earthquake engineering & structural dynamics*, 30(2) (pp. 149-171). Wiley Online Library.

[10] Ramos, L., Mevel, L., Lourenço, P.B. and De Roeck, G. (2008) Dynamic monitoring of historical masonry structures for damage identification. In: *Proc. 26th International Modal Analysis Conference*, Orlando, Florida, USA

[11] Vardanega, P.J., Webb, G.T., Fidler, P.R.A. and Middleton, C.R. (2016) Bridge monitoring. In: *Innovative Bridge Design Handbook*, (pp. 759-775). Elsevier.

[12] Brincker, R., Andersen, P. and Cantieni, R. (2001) Identification and level I damage detection of the Z24 highway bridge. In: *Experimental techniques*, 25(6) (pp. 51-57). Springer.

[13] Andersen, P. (1997) Identification of civil engineering structures using vector ARMA models. *Doctoral dissertation*, Department of Building Technology and Structural Engineering, Aalborg University, Denmark.

[14] Brincker, R. and Ventura, C. (2015) Introduction to operational modal analysis John Wiley & Sons

[15] Olsen, P., Juul, M. and Brincker, R.(2019) Condensation of the correlation functions in modal testing. In: *Mechanical Systems and Signal Processing*, 118, (pp. 377-387), Elsevier.

[16] Leys, C., Ley, C., Klein, O., Bernard, P and Licata, L (2013) Detecting outliers: Do not use standard deviation around the mean, use absolute deviation around the median. In: *Journal of Experimental Social Psychology*, 49(4) (pp. 764-766). Elsevier.

[17] Andersen, P.L. and Nielsen, S.T. (2019) OMA Based Monitoring of a Wind Loaded Structure, Appendix C.3 *Master Thesis*, Civil Engineering, Technical University of Denmark.

[18] MathWorks. Matlab 2017b. https://se.mathworks.com/products/simulink.html